

Article

Not So Robust after All: Evaluating the Robustness of Deep Neural Networks to Unseen Adversarial Attacks

Roman Garaev^{1,*}, Bader Rasheed¹  and Adil Mehmood Khan²

¹ Institute of Data Science and Artificial Intelligence, Innopolis University, Innopolis 420500, Russia; b.rasheed@innopolis.university

² School of Computer Science, University of Hull, Hull HU6 7RX, UK; a.m.khan@hull.ac.uk

* Correspondence: o.garaev@innopolis.university

Abstract: Deep neural networks (DNNs) have gained prominence in various applications, but remain vulnerable to adversarial attacks that manipulate data to mislead a DNN. This paper aims to challenge the efficacy and transferability of two contemporary defense mechanisms against adversarial attacks: (a) robust training and (b) adversarial training. The former suggests that training a DNN on a data set consisting solely of robust features should produce a model resistant to adversarial attacks. The latter creates an adversarially trained model that learns to minimise an expected training loss over a distribution of bounded adversarial perturbations. We reveal a **significant lack in the transferability of these defense mechanisms** and provide insight into the potential dangers posed by L_∞ -norm attacks previously underestimated by the research community. Such conclusions are based on extensive experiments involving (1) different model architectures, (2) the use of canonical correlation analysis, (3) visual and quantitative analysis of the neural network's latent representations, (4) an analysis of networks' decision boundaries and (5) the use of equivalence of L_2 and L_∞ perturbation norm theories.

Keywords: machine learning; deep learning; adversarial attacks



Citation: Garaev, R.; Rasheed, B.; Khan, A.M. Not So Robust after All: Evaluating the Robustness of Deep Neural Networks to Unseen Adversarial Attacks. *Algorithms* **2024**, *17*, 162. <https://doi.org/10.3390/a17040162>

Academic Editors: Ali Safaa Sadiq Al Shakarchi, Houbing Song, Ahmad Fadhil Yusof, Sushil Kumar and Omprakash Kaiwartya

Received: 14 March 2024

Revised: 14 April 2024

Accepted: 15 April 2024

Published: 19 April 2024



Copyright: © 2024 by the authors. Licensee MDPI, Basel, Switzerland. This article is an open access article distributed under the terms and conditions of the Creative Commons Attribution (CC BY) license (<https://creativecommons.org/licenses/by/4.0/>).

1. Introduction

The growth of computing power and data availability has led to the development of more efficient pattern recognition techniques, such as neural networks and deep learning. When a sample accurately represents a population of data and is of sufficient size, deep learning methods can produce impressive results, even on unseen data, making them suitable for tasks such as classification and prediction tasks. Although these methods offer significant advantages, they also come with limitations, such as the sensitivity of deep neural networks (DNNs) to data quality and sources, as well as overfitting when trained on insufficient amounts of data. However, variations in input samples from different domains or insufficient training data can still significantly affect the performance of DNNs. As DNNs are increasingly being employed in critical applications such as medicine and transportation, enhancing their robustness is essential due to the potentially severe consequences of their unpredictability.

Using adversarial attacks is one approach to examining DNNs' robustness to diverse inputs. Adversarial attacks aim to generate the smallest adversarial perturbation, i.e., a change in input, that results in a misclassification by the model.

This study investigated the abilities and drawbacks of modern defense techniques against adversarial attacks, such as adversarial and robust training. The latter refers to the hypothesis proposed by Ilyas et al. [1]. It states that adversarial attacks exploit non-robust features inherent to the data set rather than the objects in the images. According to this hypothesis, removing these features from the data set and training a model on the modified data should render adversarial attacks ineffective.

We expanded the experiments from the original paper, trained a model on robust features, and tested it on unseen attacks. Our tests revealed that models trained on robust features **are generally not resistant to L_∞ -norm perturbations**. According to our hypothesis, even if perturbations of the L_∞ - and L_2 -norms are both imperceptible to humans, L_∞ -norm attacks have a greater impact on the representations of the models.

We conducted a series of experiments and found strong evidence for our hypothesis. First, we compared the perturbations produced by different attacks utilising the theorem of vector norm equivalence in a finite-dimensional space. This comparison showed that the choice of perturbation constraints is too loose, despite being widely used in the literature. Second, by applying canonical correlation analysis, we discovered that L_∞ -norm attacks cause the most dispersion in the latent representation. Finally, we analysed the impact of robust and adversarial training methods on the decision boundary of a model. The experiment showed that an L_∞ -norm attack actually reduces the distance between the representations of a model and its decision boundary, which has a negative influence on the model generalisation.

Researchers might use our findings to develop more reliable adversarial training methods: while L_2 - and L_∞ -norm perturbations look similar, the L_∞ -norm ones are much harder to resist. To our knowledge, no one has paid so close attention to the differences between the attack norms before.

The structure of this paper is as follows: In Section 2, we present a brief overview of various attacks on image classifiers, discuss the potential defense strategies that we used in our experiments, and review the theory of robust features.

To present our massive experiments in the most convenient way, we do not separate them into methodology and results Sections. Instead of that, we group the experiments into three logical blocks. Despite being separated into different Sections, all of them serve to answer to what extent adversarial and robust training are transferable. The corresponding results follow right after the experiment descriptions. In Section 3, we challenge the generalisation of robust and adversarial training using various approaches. In Section 4, we analyse how the robustly trained models represent the adversarial and benign data samples. In Section 5, we investigate the impact of adversarial training on the decision boundaries of neural networks.

In Section 6, we discuss the possible explanation of our observations. The conclusion of our study is presented in Section 7.

2. Related Works

We focus on attacks on image classifiers, as they are the most widespread and mature; however, adversarial attacks are not limited by the type of input or task. The reader may find examples of attacks in other domains, such as malicious URL classification [2], communication systems [3], time series classification [4], malware detection in PDF files [5], etc. We suppose that an adversary has complete information about the neural network, including weights, gradients, and other internal details (white-box scenario). We also assume that in most cases, the adversary's goal is to simply cause the classifier to produce an incorrect output without specifying a particular target class (untargeted attack scenario). Other possible scenarios of adversarial attacks can be found, for example, in [6].

2.1. Adversarial Attacks

In this Subsection, we briefly describe the adversarial attacks that we used in the experiments.

2.1.1. Fast Gradient Sign Method (FGSM)

The FGSM was proposed by Goodfellow et al. in [7]. Adversarial example \tilde{x} for image x is calculated as

$$\tilde{x} = x + \epsilon \text{Sign}(\nabla_x J(x, \theta, y)) \quad (1)$$

where ϵ is the perturbation; J is the cost function for a neural network with weight θ , calculated for the input image x with true classification label y .

2.1.2. Projected Gradient Descent (PGD)

A PGD attack, introduced by Madry et al. in [8], is an iterative variant of the FGSM, carrying out a similar operation to (1) with projection on the ϵ -ball:

$$\tilde{x}^t = \pi_{x+S}(\tilde{x}^{t-1} + \epsilon \text{Sign}(\nabla_x J(x, \theta, y))) \quad (2)$$

where π is the projection of an adversarial example on the set of possible perturbations S , and t is the number of steps in iteration.

2.1.3. DeepFool

Moosavi-Dezfooli et al. [9] provided a simple iterative algorithm to perturb images to the closest wrong class. In other words, DeepFool is equal to the orthogonal projection onto the classifier's decision boundary. This property allows one to use the attack to test the robustness of a model:

$$\hat{\rho}_{adv}(f) = \frac{1}{|D|} \sum_{x \in D} \frac{\|\hat{r}\|_2}{\|x\|_2} \quad (3)$$

where $\hat{\rho}_{adv}$ is the average robustness, f is the classifier, \hat{r} is the successful perturbation from DeepFool, and D is the data set. DeepFool can be used to calculate the distance from a data point to the closest point on the decision boundary [10].

2.2. Adversarial Training as a Defense Method

One of the most popular approaches to defending neural networks against attacks is called adversarial training. It proposes "including" possible adversarial examples in the training data sets to prepare a model for attacks. To obtain an adversarially trained model, one should solve the following min-max optimisation problem [8]:

$$\arg \min_{\theta} \sum_{(x_i, y_i) \in D} \max_{\delta \in S} L(f_{\theta}(x_i + \delta), y_i) \quad (4)$$

where, θ is the weight of the neural network, D is the training data set, S is the space for possible perturbations, and $S = \{\delta : \|\delta\|_p < \epsilon\}$ for a given radius ϵ .

Adversarial training was introduced by Goodfellow et al. in [7]. Madry et al. [8] proposed using a PGD attack during the training procedure and presented better robustness against adversarial attacks. However, Wong et al. [11] achieved about the same accuracy against adversarial attacks using a simple one-step FGSM. Here and further, we refer to training based on empirical risk minimisation as "regular" since it does not involve any adversarial attack and is traditionally used to train neural networks.

It is important to note that the provable defense (i.e., "certified robust") against any small- ϵ attack has already been studied, for example, by Wong and Kolter [12] and Wong et al. [13]. However, the experiments in these works were conducted with relatively small perturbations. For example, in [13] the maximum radius of the L_{∞} perturbation is $\frac{2}{255}$, while the same norm in the adversarial training package in [14] is $\frac{8}{255}$. Thus, we do not include certified methods in our research.

2.3. Hypothesis about the Cause of Adversarial Attacks

The exact reason why neural networks are susceptible to small changes in input data remains unclear. Goodfellow et al. [7] argued that adversarial examples result from models being overly linear rather than nonlinear. However, another perspective considers poor generalisation as the source of attacks. Ilyas et al. [1] hypothesised that neural networks' vulnerability to adversarial attacks arises from their data representation. Classifiers aim to extract useful features from data to minimise a cost function. Ideally, these features

should be related to the classification objects (robust features), but neural networks may utilise unexpected properties specific to a particular data set (non-robust features). As a consequence, an adversary can utilise non-robust features that actually make no sense for human perception. If a classifier can be trained on a data set containing only robust features, it should be resistant to adversarial attacks. We refer to this process as robust training.

This hypothesis serves as an entry point for our broad research on the role of adversarial attack norms in network prediction. We challenge the robust features hypothesis for several reasons. First, it is not fully proven, except for the toy example in [1] and experiments on robust and non-robust data set creation. Second, subsequent works like [15,16] consider this hypothesis, though it might not be entirely accurate. For example, Zhang et al. [16] proposed a similar experiment, referring to [1], and developed it for universal perturbation. Although the results of [1] were discussed in [17], the accuracy of a robustly trained model was tested nowhere but in the original work, and we would like to fill this gap.

3. Generalisation of Robustly and Adversarially Trained Models

One of the goals of this work is to check the generalisation of robustly and adversarially trained models to various unseen attacks. The lack of generalisation can be critical for the users of such models who want to be sure that they respond adequately to any noisy data. In this Section, we show that, indeed, the robustly and adversarially trained models do not generalise well and highlight the cases when their performance can be compromised significantly. In the further experiments, we explain the difference between L_2 - and L_∞ -norm perturbations, which might be the cause of the lack of generalisation.

3.1. The Broad Testing of Robust and Adversarial Training

We replicated robust training from [1], employing a broader testing setup. It included various attack norms, data sets, and model architectures. The motivation for this experiment stems from the work of Tramer et al. [18], which demonstrates that even adversarially trained models could be compromised by unseen attacks; thus, they do not generalise well. We wanted to test this statement and go further by checking the generalisation of robustly trained models.

Robust training involves several steps:

1. Select an adversarially pre-trained model and the data set for image classification.
2. For each image (named “target”) from the data set, randomly generate a noisy image.
3. Compute the representations using an adversarially trained model for both the random and target images. At each iteration, slightly adjust the random image to minimise the distance between the vectors of the two images. After a set number of steps, this method produces a modified image with robust features only. So, image by image, compute a new, robust data set from the original.
4. Train the model regularly with the same architecture on this modified data set, ultimately resulting in a robustly trained model.
5. Test the generalisation capacity of both the adversarial and robust models: compute the accuracy under attacks that were not considered during the adversarial training phase and hence not used in the formation of the robust model.

Following this approach, we performed several experiments. Firstly, we took two adversarially trained ResNet50-s [19]. The training data set for the models was CIFAR-10 [20]; the training attack was PGD with L_2 - and L_∞ -norms. We tested their performance against FGSM (L_1 -, L_2 -, L_∞ -norms), PGD (L_1 -, L_2 -, L_∞ -norms), C-W (L_2 -norm), and DeepFool (L_2 -norm) attacks. A C-W attack refers to the Carlini and Wagner adversarial attack; a detailed description of it can be found in the original paper [21]. The performance results of the L_2 -trained model are outlined in Table 1, and those of the L_∞ -trained model are presented in Table 2.

Second, we performed the same experiment on the Inception V3 [22] model. For computational reasons, we only took one model, trained with a PGD attack with an L_∞ -

norm. The results are displayed in Table A1. Note that ϵ for the attacks differs from the similar ones for ResNet50-s because the model has a bigger input shape (224×224 vs. 32×32 , respectively).

Thirdly, we tried to manage the entire adversarial training pipeline ourselves from scratch. Owing to computational constraints, we selected the relatively more manageable ResNet18 architecture. The models were trained on a PGD attack with five iterations and L_2 - and L_∞ -norms. For data sets, we utilised CIFAR-10 and CINIC-10 [23] as the data sets, and PGD and FGSM as the test attacks. The results for CIFAR-10 and CINIC-10 are displayed in Tables 3 and A2, respectively.

To save space in this subsection, we put some of the tables in Appendix A and do not specifically comment on them. However, these results make the experiment more solid, confirm the overall conclusion (written in the following), and present the same patterns of adversarial and robust training as the models in Tables 1 and 2.

Table 1. Robust ResNet50 trained on L_2 data set and related adversarial model. The epsilon column stands for the budget of perturbation; the norm stands for the way of measurement for this budget; steps—maximum iterations for adversarial example creation, Robust acc.—accuracy of robustly trained model, Adv. acc.—accuracy of the corresponding adversarially trained model.

Attack	Norm	Epsilon	Steps	Robust acc.	Adv. acc.
No attack	-	-	-	0.813	0.91
FGSM	L_1	0.5	1	0.81	0.91
FGSM	L_2	0.25	1	0.59	0.87
FGSM	L_∞	0.25	1	0.1	0.13
FGSM	L_∞	0.025	1	0.22	0.62
PGD	L_1	0.5	100	0.81	0.91
PGD	L_2	0.25	1000	0.483	0.82
PGD	L_2	0.5	100	0.202	0.75
PGD	L_∞	0.025	5	0.168	0.54
PGD	L_∞	0.25	5	0.08	0.06
C-W	L_2	0.25	10	0.219	0.86
DeepFool	L_2	0.25	-	0.124	0.127

Table 2. Robust ResNet50 trained on L_∞ data set and related adversarial model.

Attack	Norm	Epsilon	Steps	Robust acc.	Adv. acc.
No attack	-	-	-	0.73	0.87
FGSM	L_1	0.5	1	0.73	0.87
FGSM	L_2	0.25	1	0.504	0.826
FGSM	L_∞	0.25	1	0.07	0.19
FGSM	L_∞	0.025	1	0.2	0.724
PGD	L_1	0.5	100	0.731	0.87
PGD	L_2	0.25	1000	0.414	0.813
PGD	L_2	0.5	100	0.195	0.663
PGD	L_∞	0.025	5	0.155	0.683
PGD	L_∞	0.25	5	0.11	0.052
C-W	L_2	0.25	10	0.51	0.81
DeepFool	L_2	0.25	-	0.13	0.111

On examination, it is apparent that adversarial and robustly trained models demonstrate reasonable stability against some variations of PGD and FGSM attacks, for example, with an L_1 -norm. However, all attacks with an L_∞ -norm significantly undermined the accuracy of the models. Hence, the model does not ensure generalisation against all attack types, primarily because a simple increase in norm or perturbation shows a drastic impact.

Table 3. Accuracy of ResNet18-s, trained on CIFAR-10 data set.

	Regular Model	Adv. Trained, L_∞ -Norm	Adv. Trained, L_2 -Norm
Accuracy on CINIC-10 (no attack)	76%	75%	72%
Accuracy on CIFAR-10 (no attack)	95%	94%	91%
Accuracy on CINIC-10 (PGD attack)	7%— L_∞ attack, 11%— L_2 attack	37%— L_∞ attack, 36%— L_2 attack	40 %— L_∞ attack, 43%— L_2 attack
Accuracy on CIFAR-10 (PGD attack)	7%— L_∞ attack, 27%— L_2 attack	57%— L_∞ attack, 55%— L_2 attack	61 %— L_∞ attack, 64 %— L_2 attack
Accuracy on CINIC-10 (FGSM attack)	49 %— L_∞ attack	67 %— L_∞ attack	66 %— L_∞ attack
Accuracy on CIFAR-10 (FGSM attack)	72 %— L_∞ attack	89 %— L_∞ attack	87 %— L_∞ attack

3.2. Equivalence of L_2 and L_∞ Perturbation Norms

To explain the lack of generalisation in the previous experiment, we used the theorem of the equivalence of vector norms on finite-dimensional spaces. The theorem states that for a given two norms $\|\cdot\|_a$ and $\|\cdot\|_b$ on the finite-dimensional vector space V over C , there exists a pair of real numbers $0 < C_1 \leq C_2$ such that, for all $x \in V$, the following inequality holds:

$$C_1 \|x\|_b \leq \|x\|_a \leq C_2 \|x\|_b \tag{5}$$

In other words, all norms are equal to each other with respect to some coefficients. Images and adversarial perturbations are finite-dimensional vectors over R ; thus, the same inequality holds for the L_2 - and L_∞ -norms. The ϵ -s that we used in the previous experiments, such as $\epsilon = 0.03$ for the L_∞ -norm and $\epsilon = 0.25$ for the L_2 -norm on the CIFAR-10 data set, are widely used [7,8]. In practice, such a choice seems reasonable because the corresponding perturbations are indistinguishable by the human eye. However, such ϵ -s might be too loose, which can explain the superiority of L_∞ -norm attacks.

1. Take the CIFAR-10 test data set and two attacks: PGD with an L_2 -norm of attack and $\epsilon = 0.25$; and PGD with an L_∞ -norm and $\epsilon = 0.03$.
2. Generate adversarial perturbations by these attacks. Save only the perturbation that misclassifies a network: the prediction of such an adversarial sample must not be equal to the true label and prediction of the original image.
3. Flatten the perturbation matrices into vectors and calculate the norms.
4. Iterating over the perturbations, take C_1 and C_2 as $C_1 = \min(\frac{x_{pert_2}}{x_{pert_\infty}})$ and $C_2 = \max(\frac{x_{pert_2}}{x_{pert_\infty}})$. Therefore, in Equation (5) we picked $a = 2$, $b = \infty$, but this was an arbitrary choice.
5. Repeat for three models: regular ResNet-50 and adversarially trained ResNets-50 with L_2 - and L_∞ -norms of attacks. In addition, for all cases, calculate the percentage of adversarial misclassified samples by the model.

The results are presented in Table 4.

Table 4. Coefficients for Equation (5). Testing attacks are PGD with L_2 and L_∞ perturbation norms; testing data set is CIFAR-10.

Model	Attack Norm					
	L_2			L_∞		
	C_1	C_2	% of Misclassified	C_1	C_2	% of Misclassified
Regular ResNet-50	4.6	14.4	86	43.6	55.4	96
Adv. trained ResNet-50 (L_2)	3.3	14.3	8	45.8	55.4	52
Adv. trained ResNet-50 (L_∞)	1.6	7.3	10	45.4	55.4	44

For generalisation purposes, we also tested the same models on an FGSM attack with $\epsilon = 0.03$ (attack norm was L_∞) and we present the results in Table 5. We also conducted the same experiment on the CINIC data set (Table 6).

Table 5. Coefficients for Equation (5). Testing attack is FGSM; the testing data set is CIFAR-10.

Model	C_1	C_2	% of Misclassified
Regular ResNet-50	41.9	55.4	36
Adv. trained ResNet-50 (L_2)	40	55.4	22
Adv. trained ResNet-50 (L_∞)	45.6	55.4	13

Table 6. Coefficients for Equation (5). Testing attacks are PGD with L_2 and L_∞ perturbation norms, the testing data set is CINIC.

Model	Attack Norm					
	L_2			L_∞		
	C_1	C_2	% of Misclassified	C_1	C_2	% of Misclassified
Regular ResNet-50	4.5	14.8	70	39.7	55.4	82
Adv. trained ResNet-50 (L_2)	4.1	15.2	12	43.3	55.4	52
Adv. trained ResNet-50 (L_∞)	1.2	7.3	15	43.5	55.4	37

From Tables 4 and 5, one can observe the following:

- The coefficients in L_∞ attacks are significantly higher than those for L_2 -norm attacks. Since the coefficients are the fractions between the norms, and $x_{pert_\infty} = 0.03$, the L_2 -norm of such perturbations is much higher than 0.25. In fact, when C_2 is approximately 55, each pixel of the perturbed image is equal to ± 0.03 .
- For L_2 attacks, on the other hand, the overall perturbation is restricted by 0.25, but some particular pixels can be changed more than 0.03. The small values of C_1 and C_2 for the L_∞ -norm adversarially trained model indicate high magnitude in some image regions.

In this experiment, we called into question the traditional choice of ϵ -s in the literature on adversarial attacks. We leave the more detailed analysis of the coefficient range for a truly robust model for further research.

3.3. Loss Distributions of the Adversarially Trained Models

To illustrate the disparity between adversarial attack norms, we took three ResNet50 models from the first experiments: one model was regularly trained on CIFAR-10, while the other two were adversarially trained by PGD attacks with L_2 - and L_∞ -norms, respectively. The performance of each model was evaluated using histogram plots, where the X-axis represents the cross-entropy loss between predictions and one-hot-encoded labels and the height of bars displays the number of samples in a given region. We used a CIFAR-10 test data set with 10,000 samples in total.

To challenge these models, we used two types of PGD attacks: the L_2 -norm of perturbation with $\epsilon = 0.5$ and the L_∞ -norm with $\epsilon = 0.05$. The number of steps for the L_∞ -norm attack was set to five, while that for the attack on L_2 was 10. Additionally, the loss of each model on clean data was assessed.

Each plot represents one model and includes three distributions: losses in clean and adversarially perturbed CIFAR-10 test data (10,000 samples), with L_2 - or L_∞ -norm attacks. The performance of each model is presented by histogram plots. The X-axis stands for the cross-entropy loss between predictions and one-hot encoded labels (lower is better). The height of bins displays the number of samples that fell in a given region. The A-distance, which is used in domain adaptation [24], additionally illustrates the difference between the

distributions of clean and adversarial samples. A higher A-distance value indicates greater dissimilarity between distributions. The plots are presented in Figures 1–3. For the better visualization, we plot kernel density estimation alongside with histogram for each attack, with the corresponding color.

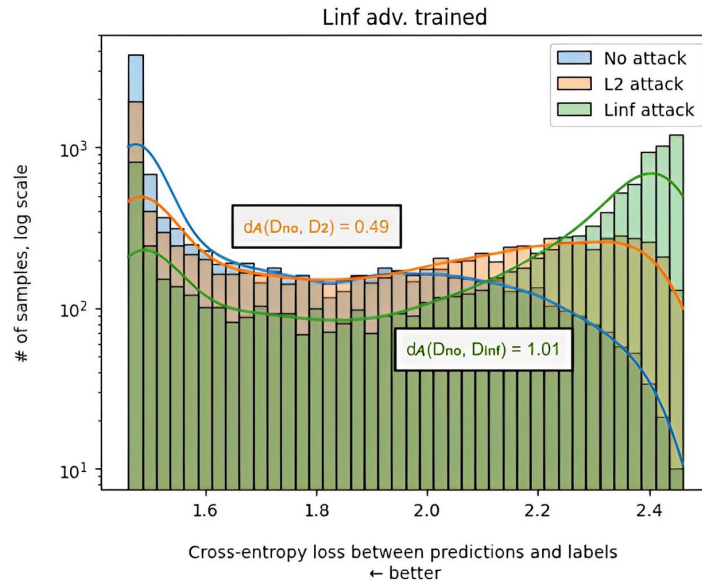


Figure 1. Distributions of samples for adversarially trained ResNet50. Training attack—PGD with L_∞ -norm, ϵ is 0.03.

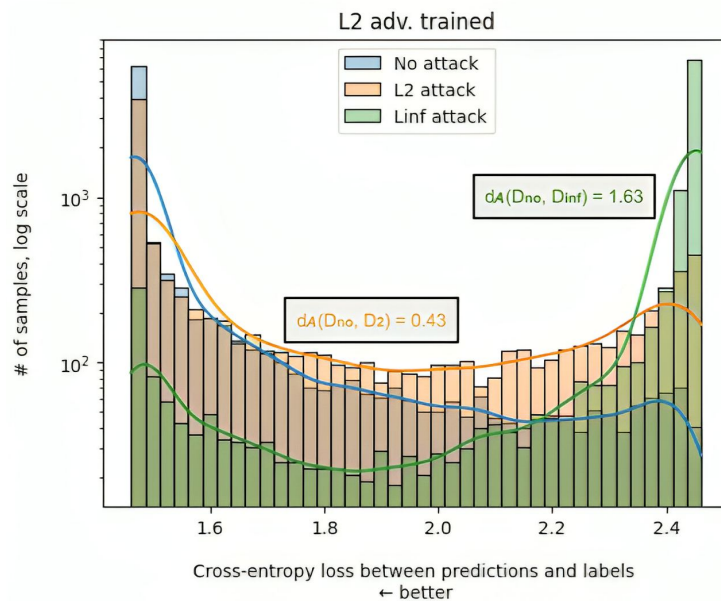


Figure 2. Distributions of samples for adversarially trained ResNet50. Training attack—PGD with L_2 -norm, ϵ is 0.5.

In all figures, the distributions of attack with an L_∞ perturbation norm (Figure 1) have a peak near the maximum loss. Although, for the regularly trained model (Figure 3), approximately all samples are located near this peak, for adversarially trained models, there are also smaller peaks on the left side of the distributions. The distributions of clean data have about the same shape on every plot: a high peak on the very left bar (mean with the least error) and a smooth decrease to the right side. The distributions of adversarial samples with the L_2 -norm (Figure 2) have a similar peak for adversarially trained models;

however, they have a more flattened tail. For the regularly trained model, most of the examples fall into the right region, as for the attack with the L_∞ -norm (note the scale).

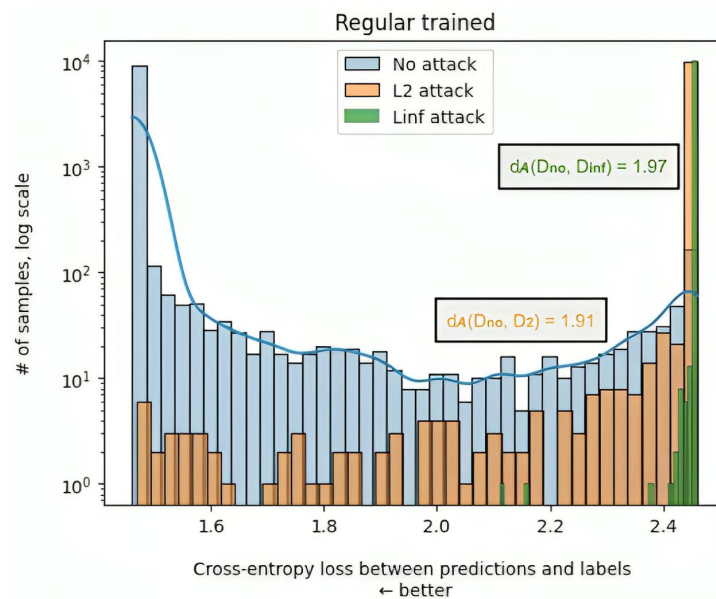


Figure 3. Distributions of samples for regularly trained ResNet50.

The results indicate that adversarial attacks alter the shape of the sample distribution, with the norms of attack playing a significant role in determining the curves' appearance. The A-distance confirms this finding. Adversarial training brings the adversarial and benign distributions closer together but does not achieve complete convergence, particularly for attacks with an L_∞ -norm.

4. Analysis of the Representations

We extend the research on adversarial and robust training. While in the previous Section we focused mostly on attack parameters and perturbations, we are also interested in how a model represents benign and adversarial samples. We aim to determine the proximity of such representations for a robustly trained model. The degree of similarity between representations of samples with small L_∞ - or L_2 -norms indicates the stability of a model. We analysed the representations of neural networks from the robust training experiment (Section 3.1) using singular value canonical correlation analysis and performed a principal component analysis for their visualisation.

4.1. Comparison of Representations under Adversarial Attacks

Canonical correlation analysis (CCA) is a method used to compare the representations of neural networks. Its objective is to identify linear combinations of two sets of random variables that maximise their correlation. CCA has been employed to compare activations from different layers of neural networks, for example, by Morcos et al. [25] and An et al. [26]. Raghu et al. [27] proposed an extension of CCA, singular value canonical correlation analysis (SVCCA), for neural network analysis.

We employed SVCCA to compare the representations of the original and corresponding adversarial images. For each experiment, we took a batch of 128 images, computed the related adversarial examples under some attack, calculated the SVCCA for the representations, and took the mean. In each experiment, we tested the same models as in the previous experiments: a regularly and two adversarially trained ResNet50-s. In this experiment, a high mean correlation coefficient indicated that the representations were similar to each other and that small perturbations did not impact the model.

Although attack norms were the primary variables in these experiments, we also tested two different attacks (FGSM and PGD) to eliminate the threat of validity. The means of SVCCA are presented in Table 7. The results of the same for the best and worst cases from Tables 1 and 2 in Table A3 can be found in Appendix B.

Table 7. Mean correlation coefficient for different models. The values of the lowest mean correlation coefficients for each model are bold.

Attack	Parameters	Regular Model	Adv. Trained, L_2	Adv. Trained, L_∞
PGD	$L_2, \epsilon = 0.25, steps = 100$	0.686	0.981	0.989
	$L_\infty, \epsilon = 0.025, steps = 100$	0.587	0.751	0.822
FGSM	$L_2, \epsilon = 0.25$	0.833	0.982	0.991
	$L_\infty, \epsilon = 0.025$	0.618	0.78	0.837

The results in Tables 7 and A3 demonstrate that adversarial attacks with L_∞ -norm perturbation have the most significant impact on the representations. This effect is evident even in models that were trained specifically to handle L_∞ -norm attacks. These findings emphasise the importance of considering adversarial attack norms when evaluating model robustness because testing in the L_2 -norm may provide a false sense of security.

4.2. Visualisation of Representations

The visualisation of representations presents a challenge due to the high dimensionality of representation vectors. Nonetheless, such visualisation can be useful for analysis purposes. To address this issue, we employed principal component analysis (PCA) to reduce the dimensionality of representations from 512 to 2. We limited our experimentation to ResNet18 due to computational constraints.

We present the visualisation of representations for different combinations of models and norms of PGD attacks in Figures 4–8. Figure 4 depicts the representations of samples from CIFAR-10 for a regularly trained ResNet18, which serves as a baseline case. In Figures 5 and 6, we visualise the data as adversarial samples with L_2 - and L_∞ -norms of attack, respectively. Furthermore, we examine the representations of adversarial samples for adversarially trained models in Figures 7 and 8. To challenge the models, we use alter norms of attacks from training ones: the model trained on PGD with an L_2 -norm is tested on an L_∞ -norm PGD (Figure 8), and vice versa (Figure 7). We group the representations of different classes by colours in all figures to comprehend how the representations of different classes intermingle under adversarial attacks.

The representations of the regularly trained networks are clustered according to the classes in the data set, as shown in Figure 4. However, when subjected to adversarial attacks, all representations become heavily mixed, resulting in a more challenging classification task due to overlapping representations of different classes. The most mixed representations were observed on the regularly trained network through the L_∞ -norm PGD attack (Figure 6). On the contrary, adversarial training, as shown in Figures 7 and 8, resulted in some class representations (e.g., “Automobile” or “Truck”) remaining clustered while becoming closer to each other than those without attacks. The same pattern was observed for the L_2 -norm attack (Figure 6).

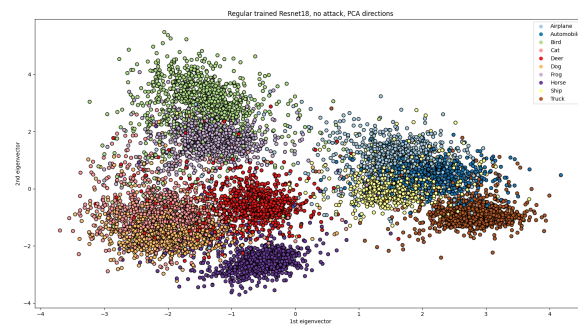


Figure 4. Representations of regularly trained ResNet18 on clean data set (CIFAR-10).

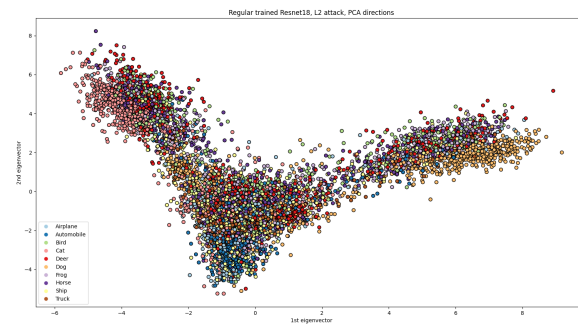


Figure 5. Representations of regularly trained ResNet18 on adversarial data set (CIFAR-10), PGD with L_2 -norm and 20 steps.

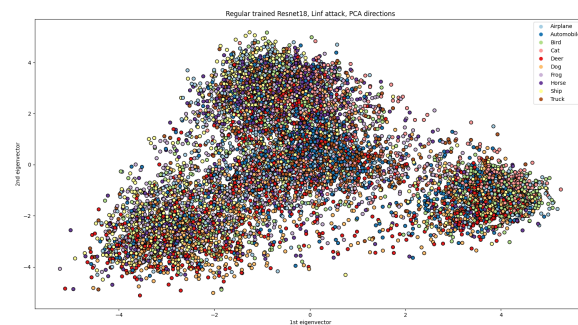


Figure 6. Representations of regularly trained ResNet18 on adversarial data set (CIFAR-10), PGD with L_∞ -norm and 20 steps.

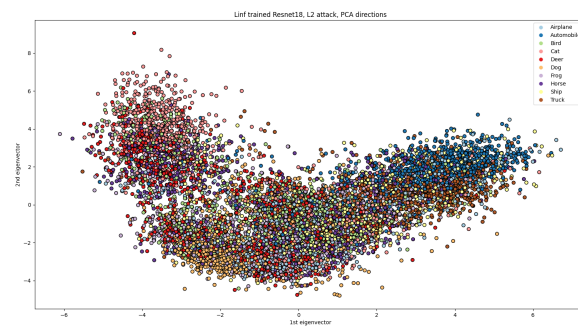


Figure 7. Representations of adversarially trained ResNet18 (PGD, L_∞ -norm) on adversarial data set (CIFAR-10), PGD with L_2 -norm and 20 steps.

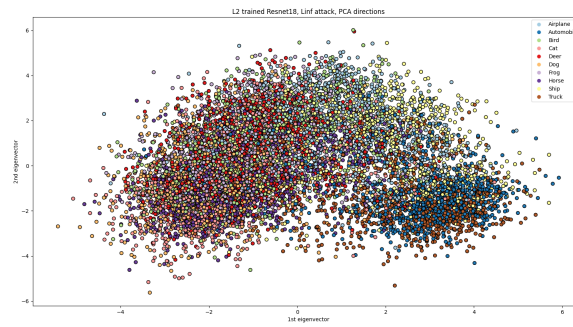


Figure 8. Representations of adversarially trained ResNet18 (PGD, L_2 -norm) on adversarial data set (CIFAR-10), PGD with L_∞ -norm and 20 steps.

5. Impact of Adversarial Training on the Network’s Decision Boundary

As a continuation of generalisation testing, we aim to investigate the impact of robust and adversarial training methods on the decision boundary of a model. Particularly, we show how the mean distance between samples and decision boundaries varies for different models when exposed to adversarial attacks.

We use the idea of Mickisch et al. [10], who utilised the DeepFool attack in Section 2.1.3 to measure this distance. The decision boundary is defined as the set of input images where two or more classes share the same maximum probability, indicating that the classifier is uncertain about the class of the image:

$$D = \{x \in R^n | \exists k_1, k_2 = 1 \dots c, k_1 \neq k_2, f(x)_{k_1} = f(x)_{k_2} = \max(f(x))\} \tag{6}$$

where c is the number of classes. Under this definition, the usage of the DeepFool attack looks natural because it aims to find a perturbation to the closest wrong class. The distance of the sample x to the decision boundary D can be measured as

$$d(x) = \min \epsilon, s.t. x + \epsilon \in D \tag{7}$$

The pre-trained ResNet50 model is used with 20 steps of PGD attack during training, while ResNet18 models are trained under PGD with only 5 steps. The test data set is CIFAR-10. The outputs of the ResNet18 and ResNet50 models with different training configurations are presented in Table 8. The table displays the mean difference between the decision boundaries of models and images from CIFAR-10, calculated using the L_2 distance. The “steps” column represents the mean iteration of DeepFool spent during the attack generation. A comparison is made between the models in Tables 1–3.

Table 8. Mean distance of samples to decision boundary.

Model	Mean L_2 Distance	Steps
Regularly trained ResNet18	0.1793	1.92
Adversarially trained ResNet18 (L_2 -norm)	0.659	1.98
Adversarially trained ResNet18 (L_∞ norm)	0.1018	2.5
Regularly trained ResNet50	0.17	2.58
Adversarially trained ResNet50 (L_2 -norm)	1.3728	1.77
Adversarially trained ResNet50 (L_∞ -norm)	1.18	2.66

The results indicate that the mean distance for ResNet18-s (for all types of training) from the decision boundary is relatively small, especially for the L_∞ -norm. A small distance from a sample to the decision boundary implies that it is easier to misclassify this sample because it does not require a significant perturbation. Interestingly, the distance for

the L_∞ -norm adversarially trained model is actually less than training ϵ . However, the testing of this model under PGD attack (Table 3) suggests that it has some robustness. Therefore, the reliability of the popular method of model testing used in this study is called into question.

6. Discussion

One explanation for the robustness difference between L_∞ -norm and L_2 -norm attacks is according to the adversarial purification framework in Allen-Zhu and Li [28]. In this context, L_∞ -norm attacks typically manipulate an image by applying the maximum allowable perturbation to each pixel within the defined infinity norm constraint. This kind of attack can exploit the dense mixtures in non-purified features more uniformly across all dimensions of the input space. L_2 -norm attacks, on the other hand, distribute their perturbations more smoothly and are constrained by the Euclidean distance. This form of attack could be more aligned with the types of perturbations that adversarial training with feature purification is specifically designed to defend against, as the training process aims to stabilize the model against perturbations that have a concentrated energy in the feature space.

7. Conclusions

While strong adversarial attacks on neural networks have already been developed, most of the defense mechanisms still do not guarantee full resistance to them in general. In this study, we consider the impact of adversarial and robust training on a model's ability to adequately represent adversarial samples. The experiments demonstrate that the model, trained on a "robust" data set, is still vulnerable to some attacks; thus, adversarial attacks do not compromise only non-robust features. Thus, the robust features are not well generalised, especially on the L_∞ -norm of attack. We assume that the small difference between clean and adversary inputs for the L_∞ attack leads to a huge gap in the latent space between them; SVCCA of different attack representations confirms this assumption. Our visualisation of neural network representation also shows the difference between L_2 - and L_∞ -norms of attack. Moreover, we discover that L_∞ -norm adversarial training decreases the distance between the representations and the decision boundary.

In light of these results, we recommend that researchers in the field of adversarial attacks and defense mechanisms pay closer attention to L_∞ -norm attacks to avoid a false sense of security. It is crucial to consider this norm in their tests to ensure the robustness of models against potential attacks. As the next step in this research, we would like to determine the perturbation coefficient range (experiment in Section 3.2) that should be reasonable for a robust model.

Author Contributions: Conceptualization, A.M.K. and R.G.; methodology, A.M.K. and R.G.; software, R.G.; validation, B.R.; writing—original draft preparation, R.G.; writing—review and editing, A.M.K. and B.R.; supervision, A.M.K. All authors have read and agreed to the published version of the manuscript.

Funding: This research received no external funding.

Data Availability Statement: The code of our implementation of for robust networks training is available on [github](#).

Conflicts of Interest: The authors declare no conflict of interest.

Appendix A. Broad Test of Robust and Adversarial Training

Table A1. Robust InceptionV3 trained on L_∞ data set.

Attack	Norm	Epsilon	Steps	Robust acc.	Adv. acc.
No attack	-	-	-	0.89	0.94
FGSM	L_2	0.25	1	0.49	0.83
FGSM	L_∞	0.25	1	0.10	0.415
FGSM	L_∞	0.025	1	0.63	0.79
PGD	L_2	100	5	0.87	0.912
PGD	L_2	45	100	0.88	0.903
PGD	L_2	0.5	100	0.89	0.94
PGD	L_∞	0.5	5	0.06	0.378
PGD	L_∞	1.0	5	0.04	0.281
C-W	L_2	0.25	10	0.51	0.85
DeepFool	L_2	0.25	-	0.48	0.784

Table A2. Accuracy of ResNet18-s, trained on CINIC-10 data set.

	Regular Model	Adv. Trained, L_∞ -Norm	Adv. Trained, L_2 -Norm
Accuracy on CINIC-10 (no attack)	86 %	84 %	80 %
Accuracy on CIFAR-10 (no attack)	94 %	93 %	90 %
Accuracy on CINIC-10 (PGD attack)	3%— L_∞ attack, 6%— L_2 attack	33%— L_∞ attack, 30%— L_2 attack	42%— L_∞ attack, 46%— L_2 attack
Accuracy on CIFAR-10 (PGD attack)	4%— L_∞ attack, 7%— L_2 attack	45%— L_∞ attack, 41%— L_2 attack	55%— L_∞ attack, 59%— L_2 attack
Accuracy on CINIC-10 (FGSM attack)	50%— L_∞ attack	75%— L_∞ attack	73%— L_∞ attack
Accuracy on CIFAR-10 (FGSM attack)	63%— L_∞ attack	87%— L_∞ attack	85%— L_∞ attack

Appendix B. SVCAA

Table A3. Mean correlation coefficient for the best and worst cases in Tables 1 and 2.

Attack	Parameters	Regular Model	Adv. Trained, L_2	Adv. Trained, L_∞
PGD, best	$L_2, \epsilon = 0.25,$ $steps = 1000$	0.682	0.989	0.99
PGD, worst	$L_\infty, \epsilon = 0.25, steps = 5$	0.46	0.532	0.598
FGSM, best	$L_2, \epsilon = 0.25$	0.833	0.982	0.991
FGSM, worst	$L_\infty, \epsilon = 0.25$	0.422	0.346	0.411

References

- Ilyas, A.; Santurkar, S.; Tsipras, D.; Engstrom, L.; Tran, B.; Madry, A. Adversarial Examples Are Not Bugs, They Are Features. In Proceedings of the Advances in Neural Information Processing Systems 32: Annual Conference on Neural Information Processing Systems 2019, NeurIPS 2019, Vancouver, BC, Canada, 8–14 December 2019; pp. 125–136.
- Rasheed, B.; Khan, A.; Kazmi, S.; Hussain, R.; Jalil Piran, M.; Suh, D. Adversarial Attacks on Featureless Deep Learning Malicious URLs Detection. *Comput. Mater. Contin.* **2021**, *680*, 921–939. [[CrossRef](#)]
- Kim, B.; Sagduyu, Y.E.; Davaslioglu, K.; Erpek, T.; Ulukus, S. Channel-Aware Adversarial Attacks Against Deep Learning-Based Wireless Signal Classifiers. *IEEE Trans. Wirel. Commun.* **2020**, *21*, 3868–3880. [[CrossRef](#)]
- Karim, F.; Majumdar, S.; Darabi, H. Adversarial Attacks on Time Series. *IEEE Trans. Pattern Anal. Mach. Intell.* **2019**, *43*, 3309–3320. [[CrossRef](#)]
- Biggio, B.; Corona, I.; Maiorca, D.; Nelson, B.; Šrndić, N.; Laskov, P.; Giacinto, G.; Roli, F. Evasion attacks against machine learning at test time. In Proceedings of the Machine Learning and Knowledge Discovery in Databases: European Conference, ECML PKDD 2013, Prague, Czech Republic, 23–27 September 2013; Proceedings, Part III 13; Springer: Berlin/Heidelberg, Germany, 2013; pp. 387–402.

6. Chakraborty, A.; Alam, M.; Dey, V.; Chattopadhyay, A.; Mukhopadhyay, D. Adversarial Attacks and Defences: A Survey. *arXiv* **2018**, arXiv:1810.00069.
7. Goodfellow, I.J.; Shlens, J.; Szegedy, C. Explaining and Harnessing Adversarial Examples. In Proceedings of the 3rd International Conference on Learning Representations, ICLR 2015, San Diego, CA, USA, 7–9 May 2015 .
8. Madry, A.; Makelov, A.; Schmidt, L.; Tsipras, D.; Vladu, A. Towards Deep Learning Models Resistant to Adversarial Attacks. In Proceedings of the 6th International Conference on Learning Representations, ICLR 2018, Vancouver, BC, Canada, 30 April–3 May 2018.
9. Moosavi-Dezfooli, S.M.; Fawzi, A.; Frossard, P. DeepFool: A Simple and Accurate Method to Fool Deep Neural Networks. In Proceedings of the 2016 IEEE Conference on Computer Vision and Pattern Recognition (CVPR), Las Vegas, NV, USA, 27–30 June 2016; pp. 2574–2582.
10. Mickisch, D.; Assion, F.; Greßner, F.; Günther, W.; Motta, M. Understanding the Decision Boundary of Deep Neural Networks: An Empirical Study. *arXiv* **2020**, arXiv:2002.01810.
11. Wong, E.; Rice, L.; Kolter, J.Z. Fast is better than free: Revisiting adversarial training. In Proceedings of the 8th International Conference on Learning Representations, ICLR 2020, Addis Ababa, Ethiopia, 26–30 April 2020 .
12. Wong, E.; Kolter, Z. Provable defenses against adversarial examples via the convex outer adversarial polytope. In Proceedings of the International Conference on Machine Learning, PMLR, Stockholm Sweden, 10–15 July 2018; pp. 5286–5295.
13. Wong, E.; Schmidt, F.R.; Metzen, J.H.; Kolter, J.Z. Scaling provable adversarial defenses. *arXiv* **2018**, arXiv:1805.12514.
14. Engstrom, L.; Ilyas, A.; Salman, H.; Santurkar, S.; Tsipras, D. Robustness (Python Library). 2019. Available online: <https://github.com/MadryLab/robustness> (accessed on 13 March 2024)
15. Salman, H.; Ilyas, A.; Engstrom, L.; Kapoor, A.; Madry, A. Do adversarially robust imagenet models transfer better? *Adv. Neural Inf. Process. Syst.* **2020**, *33*, 3533–3545.
16. Zhang, C.; Benz, P.; Imtiaz, T.; Kweon, I.S. Understanding adversarial examples from the mutual influence of images and perturbations. In Proceedings of the IEEE/CVF Conference on Computer Vision and Pattern Recognition, Seattle, WA, USA, 14–19 June 2020; pp. 14521–14530.
17. Engstrom, L.; Gilmer, J.; Goh, G.; Hendrycks, D.; Ilyas, A.; Madry, A.; Nakano, R.; Nakkiran, P.; Santurkar, S.; Tran, B.; et al. A Discussion of ‘Adversarial Examples Are Not Bugs, They Are Features’. *Distill* **2019**, *4*. [[CrossRef](#)]
18. Tramèr, F.; Kurakin, A.; Papernot, N.; Goodfellow, I.J.; Boneh, D.; McDaniel, P.D. Ensemble Adversarial Training: Attacks and Defenses. 6th International Conference on Learning Representations, ICLR 2018, Vancouver, BC, Canada, 30 April–3 May 2018.
19. He, K.; Zhang, X.; Ren, S.; Sun, J. Deep residual learning for image recognition. In Proceedings of the IEEE Conference on Computer Vision and Pattern Recognition, Las Vegas, NV, USA, 27–30 June 2016; pp. 770–778.
20. Krizhevsky, A.; Hinton, G. Learning Multiple Layers of Features from Tiny Images. 2009. Available online: <https://www.cs.toronto.edu/~kriz/cifar.html> (accessed on 13 March 2024)
21. Carlini, N.; Wagner, D.A. Towards Evaluating the Robustness of Neural Networks. In Proceedings of the 2017 IEEE Symposium on Security and Privacy (SP), San Jose, CA, USA, 22–26 May 2017; pp. 39–57.
22. Szegedy, C.; Vanhoucke, V.; Ioffe, S.; Shlens, J.; Wojna, Z. Rethinking the inception architecture for computer vision. In Proceedings of the IEEE Conference on Computer Vision and Pattern Recognition, Las Vegas, NV, USA, 27–30 June 2016 ; pp. 2818–2826.
23. Darlow, L.N.; Crowley, E.J.; Antoniou, A.; Storkey, A.J. Cinc-10 is not imagenet or cifar-10. *arXiv* **2018**, arXiv:1810.03505.
24. Han, C.; Lei, Y.; Xie, Y.; Zhou, D.; Gong, M. Visual domain adaptation based on modified A-distance and sparse filtering. *Pattern Recognit.* **2020**, *104*, 107254. [[CrossRef](#)]
25. Morcos, A.; Raghu, M.; Bengio, S. Insights on representational similarity in neural networks with canonical correlation. *Adv. Neural Inf. Process. Syst.* **2018**, *31*, 5727–5736.
26. An, S.; Bhat, G.; Gumussoy, S.; Ogras, Ü.Y. Transfer Learning for Human Activity Recognition Using Representational Analysis of Neural Networks. *ACM Trans. Comput. Healthc.* **2020**, *4*, 1–21. [[CrossRef](#)]
27. Raghu, M.; Gilmer, J.; Yosinski, J.; Sohl-Dickstein, J. Svcca: Singular vector canonical correlation analysis for deep learning dynamics and interpretability. *Adv. Neural Inf. Process. Syst.* **2017**, *30*, 6078–6087.
28. Allen-Zhu, Z.; Li, Y. Feature Purification: How Adversarial Training Performs Robust Deep Learning. In Proceedings of the 2021 IEEE 62nd Annual Symposium on Foundations of Computer Science (FOCS), Denver, CO, USA, 7–10 February 2022; pp. 977–988.

Disclaimer/Publisher’s Note: The statements, opinions and data contained in all publications are solely those of the individual author(s) and contributor(s) and not of MDPI and/or the editor(s). MDPI and/or the editor(s) disclaim responsibility for any injury to people or property resulting from any ideas, methods, instructions or products referred to in the content.